31. PALEOMAGNETIC RESULTS FROM DEEP SEA DRILLING PROJECT LEG 78A[1]

Douglas S. Wilson, Geophysics Department, Stanford University[2]

ABSTRACT

The results of paleomagnetic studies of samples from DSDP Leg 78A are reported. For Site 541, the interval from 60 to 200 m sub-bottom was correlated with the Matuyama through Gilbert polarity epochs. For Site 543, the interval from 150 to 190 m sub-bottom was correlated with marine magnetic Anomalies 5C through 5E. Down-dip directions of tilted beds inferred from declination values for Sites 541 and 542 suggest a pattern of monoclinal folding. Results from basalt samples are comparable to those from other DSDP sites in relatively old basalts.

INTRODUCTION

The primary objective of Deep Sea Drilling Project Leg 78A was to study the accretionary processes of the Barbados Ridge, at the convergent margin between the American and Caribbean plates. Site locations are shown in Figure 1. Sites 541 and 542 are near the toe of the accretionary prism and about a kilometer apart; coring at both recovered only sediment and failed to penetrate the interplate thrust fault. Site 543 was chosen as a reference east (seaward) of the deformation front, on presumably normal, undeformed ocean crust; drilling there bottomed in basalt overlain by and interbedded with Upper Cretaceous (Campanian) sediments. Because of time constraints, rotary coring was used throughout the cruise.

Paleomagnetic sampling on Leg 78A was carried out with three objectives in mind: to help determine age by polarity stratigraphy; to constrain *in situ* structure with estimates of bed strikes; and to characterize the magnetic properties of the basaltic basement, thereby supplementing data from other DSDP legs on the general nature of the source layer for marine magnetic anomalies. Recovery at all the sites was fairly high, but practical considerations limited the number of sediment samples suitable for paleomagnetic work. To avoid problems with drilling disturbance or rotation resulting from undetected tectonic tilting, samples were taken only at visible beds. The drilling disturbance was sufficiently severe in the upper 50 m or so of each hole that no samples were taken in the upper parts of any of the holes. At best, the sample interval was 1–2 m, with occasional gaps of several meters or more owing to lack of recovery or the disturbed nature of the core. In Hole 541, because of the exceptionally high sediment accumulation rate, this rather sparse sample interval was adequate for polarity stratigraphy over much of the hole.

METHODS

In the less consolidated sediments of the core, samples were taken by pressing 2.4 cm × 2.4 cm × 2 cm plastic cubes into the core. The cubes, scribed with arrows pointing upcore, were pried from the rest of the core. In the more consolidated regions, an upcore arrow was scribed directly on the core, and a sample of measurable size was sawn or drilled. The basalt samples were standard 2.5 cm × 2.5 cm cores. The samples were measured on the shipboard Digico fluxgate spinner magnetometer; alternating-field (AF) demagnetization studies were carried out using the Schonstedt AF demagnetizer. For some of the specimens, follow-up studies were done at Stanford University on the Superconducting Technology two-axis cryogenic magnetometer with built-in AF demagnetizer. For the shipboard measurements, the most straightforward procedure was to imagine a hypothetical arrow on the top (upcore side) of each specimen pointing to the actual upcore arrow scribed on the side of the sample. The hypothetical arrow corresponds to the fiducial line referred to in the Digico manual, and allows the samples to be measured without using the time-consuming field or bedding corrections. The Digico convention defines the coordinate system for relative declinations: the direction normal to and away from the cut surface of the working half of the core is 0°, increasing clockwise looking downcore. In this coordinate system, the working half of the core is the "south" half. This same coordinate system was used to record strikes and dips of bedding for structural analysis. At each measurable bed, the core was sliced to give apparent dips in two different planes, defining the bedding plane. The strike of the bed was taken to be the line in the bedding plane normal to the axis of the core. By convention, the strikes recorded are 90° counterclockwise from the down-dip direction. The magnetization directions are corrected for bedding by rotating the direction about the strike line by the amount of the dip.

The measurement results are tabulated in Table 1, which lists, for each sample, natural remanent magnetization (NRM) (in A/m), magnetization at optimum demagnetization level (A/m), optimum demagnetization level (mT), polarity interpretation (normal or reversed), and reliability estimate. For samples taken at dipping beds, a second line gives strike, dip, and corrected inclinations and declinations. For the basalt samples, susceptibility (cgs) is listed instead of polarity and reliability. The reliability categories are modeled after U.S. academic course grades: A represents a stable magnetization inferred from at least two demagnetizations; B indicates that stable magnetization was inferred from the agreement between a single demagnetization and the NRM; C indicates that the magnetization direction was still changing systematically at the highest demagnetization used; D indicates a marginally stable sample; and F indicates an unstable one. The H designation indicates that the magnetization was too close to horizontal to determine the polarity. the latitude for the sites is 15°N, which should be valid for the entire Neogene. This latitude predicts a dipole inclination of 28°, which is far enough from horizontal for polarity interpretation, but shallow enough that some horizontal magnetizations should be expected either from normal secular variation or from an increase in scatter caused by rotary coring. On this basis, a sample with a stable inclination greater than +10° was judged to be normal and less than −10° was considered reversed. Inclinations between +10° and −10° were not used for polarity determinations. The expected inclination for older times is not clear, and depends on whether the sites have been on the North American Plate or South American Plate. (The active boundary between these two plates has never been clearly recognized.)

[1] Biju-Duval, B., Moore, J. C., et al., *Init. Repts. DSDP*, Vol. 78A: Washington (U.S. Govt. Printing Office).

[2] Address: Geophysics Department, Stanford University, Stanford, CA 94305.

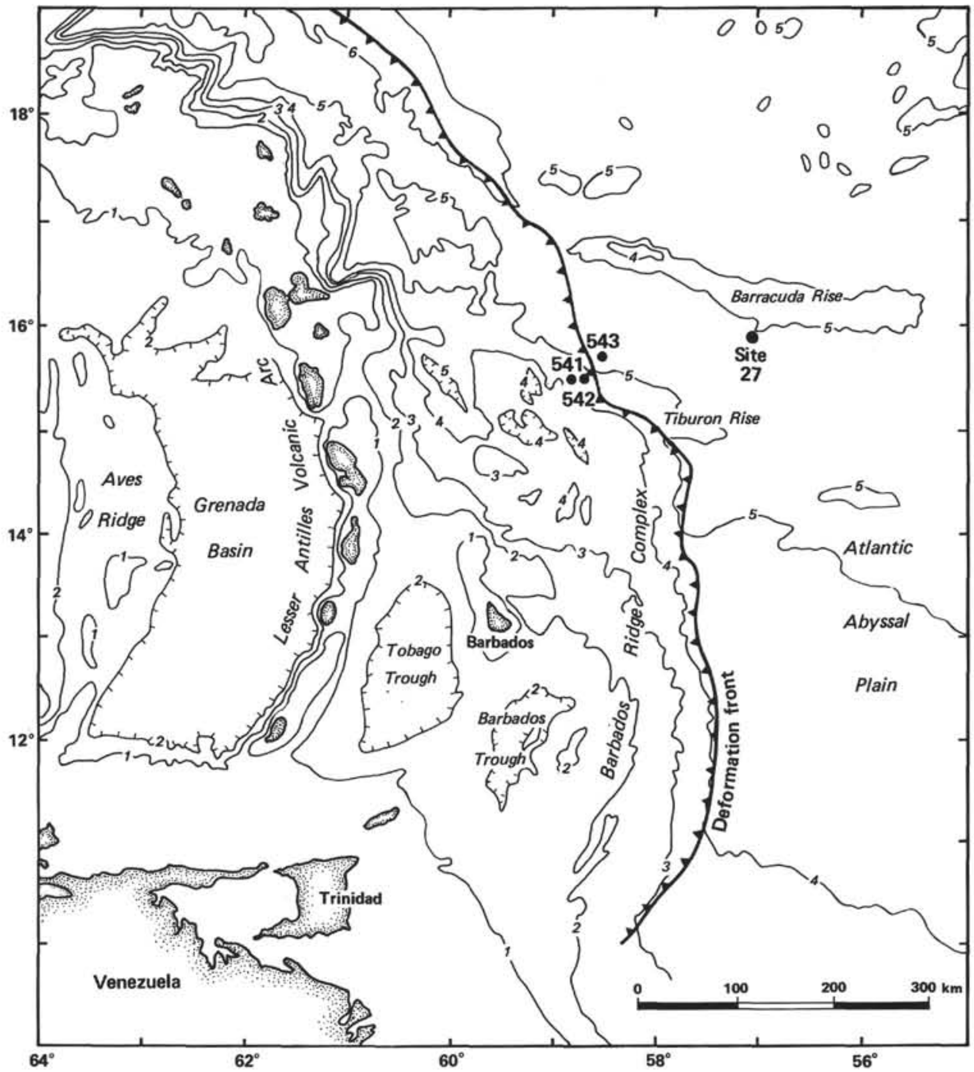

Figure 1. Locations of Sites 541, 542, and 543 on and near the Barbados Ridge.

Since the only reliable inclinations in the older samples are from the basalts, where secular variation has not been adequately averaged and tectonic tilting is probably significant, this problem has not been considered further.

POLARITY STRATIGRAPHY

Site 541

The sedimentary section at site 541 (Hole 541) yielded by far the most success in terms of polarity stratigraphy, with good determinations for the interval from 59 to 200 m sub-bottom (Cores 8 to 22; see Fig. 2). (All depths hereafter are sub-bottom.) The first sample (B-1, 141 cm; 59.4 m) is normal, corresponding to either the oldest Brunhes (0.7 Ma) or the Jaramillo event (0.91–0.97 Ma; ages are from Ness et al., 1980). Other recognizable markers are the Olduvai event (1.66–1.87 Ma) at 88–90 m (Sections 11-2 and 11-3), the Matuyama/Gauss transition (2.47 Ma) at 120.5 m (Section 14-4), and the Gauss/Gilbert transition (3.40 Ma) at about 141 m (Section 16-6). The identification of the Olduvai event corresponds extremely well to the Pliocene/Pleistocene boundary at 90–91 m (Section 11-3), identified from both nannofossils and foraminifers (Site Report for Site 541, this volume). The first normal event in the Gilbert epoch (3.86 Ma) occurs at 156 m (Section 18-3), and if there is a fault at the base of Core 19 (172 m), as indicated by an inversion in the nannofossil stratigraphy (see Site Report), the polarity information would indicate about 20 m of repeated section, with the first normal event in the Gilbert occurring again at 178 m (Section 20-5). This correlation is consistent with the two thick ash beds in Core 18 (18-1, 140 cm [154.4 m] and 18-2, 135 cm [155.8 m]) being equivalent to the two thick beds in Core 20 (20-1, 119 cm [173.2 m] and 20-3, 15 cm [175.2 m]). The polarity transition at 195 m (Section 22-3) probably corresponds to the last normal event in the Gilbert (4.79 Ma). It is very unfortunate that operational constraints prevented the use of the hydraulic piston corer, since the exceptionally high sediment accumulation rate, the reasonable magnetic stability, and the presence of datable ashes provide one of the best known opportunities to study polarity subchrons and excursions in the Brunhes and Matuyama polarity epochs.

From 289 to 340 m (Cores 32 to 37) a high percentage of the samples were horizontally magnetized, and the

Table 1A. Sediment paleomagnetic data summary.

Sample (core-section, cm level)	Sub-bottom depth (m)	NRM Inclination (degrees)	NRM Relative declination (degrees)	NRM Intensity ×10^{-3} (A/m)	Optimum Demag Inclination (degrees)	Optimum Demag Relative declination (degrees)	Optimum Demag Intensity ×10^{-3} (A/m)	Demagnetization level (mT)	Polarity	Reliability[a]
Hole 541										
8-1, 141	59.41	47	232	3.0	33	222	1.0	20	N	A
8-2, 36	59.86	6	312	1.7	−20	244	3.6	16	R	A
8-5, 14	64.14	8	331	7.9	−3	330	4.9	24	?	A/H
8-7, 13	67.13	−12	55	5.8	−14	59	4.7	16	R	A
8-7, 64	67.64	−12	73	4.8	−22	63	4.3	10	R	A
9-7, 51	77.01	11	182	4.0	−7	112	3.2	20	R?	C/H
10-1, 91	77.91	−26	41	2.4	−32	31	3.6	10	R	A
10-3, 123	81.23	−3	147	10.0	−13	148	8.5	10	R	B
10-4, 67	82.17	−34	350	2.3	−63	323	1.3	10	R	C
10-6, 125	85.75	2	22	14.8	−6	32	9.4	20	?	A/H
10-7, 47	86.47	−43	30	0.6	−20	116	0.8	20	R	C
11-1, 146	87.96	−8	188	9.7	−11	191	5.0	16	R	A
11-2, 20	88.20	28	133	3.4	33	134	1.7	13	N	A
11-2, 102	89.02	−5	32	6.3	−5	35	4.0	16	?	A/H
11-3, 17	89.67	17	96	14.4	31	107	7.7	16	N	A
11-3, 127	90.77	−3	300	3.7	−2	297	2.3	13	?	A/H
11-4, 5	91.05	−12	126	2.1	−26	100	1.6	13	R	C
11-4, 73	91.73	−8	224	6.0	−8	224	6.0	13	R	A
11-4, 110	92.10	−6	233	6.9	−16	229	6.1	13	R	A
12-1, 22	96.22	−54	272	4.3	−59	259	3.0	13	R	A
12-7, 22	105.22	?	164	7.9	−14	165	4.3	13	R	A
12-7, 70	105.70	13	161	0.8	−17	158	1.7	13	R	C
13-1, 77	106.27	−24	128	12.0	−24	134	13.0	13	R	A
13-3, 103	109.53	−28	104	2.1	−31	137	2.8	13	R	C
13-4, 113	111.13	−11	145	4.8	−6	147	2.9	16	?	A/H
13-5, 65	112.15	1	317	6.5	1	312	3.9	16	?	A/H
13-5, 135	112.85	4	357	8.2	2	359	5.6	13	?	A/H
13-6, 89	113.89	−15	78	3.0	−30	103	3.1	13	R	C
13-7, 60	115.10	−6	248	3.5	−15	233	3.5	16	R	A
14-1, 40	115.40	−38	210	0.8	−34	190	1.5	16	R	A
14-1, 116	116.16	36	177	0.47	6	157	0.27	16	?	A/H
14-2, 61	117.11	−32	101	4.8	−21	107	3.9	16	R	A
14-2, 132	117.82	−3	149	4.5	2	147	3.8	16	?	B/H
14-3, 150	118.50	−35	336	1.3	−36	330	1.6	16	R	A
14-3, 121	119.21	29	5	2.7	6	39	1.2	30	?	A/H
14-4, 10	119.60	−4	120	8.4	−6	126	4.3	23	?	A/H
14-4, 70	120.20	−26	178	4.8	−46	182	3.4	23	R	A
14-4, 141	120.91	9	180	4.4	10	183	3.7	13	N	A
14-5, 54	121.54	3	316	7.9	−1	328	5.4	16	?	A/H
14-6, 56	123.06	30	104	12.7	26	106	7.6	16	N	A
14-6, 120	123.70	3	113	7.7	3	99	2.9	25	?	A/H
14-7, 60	124.50	3	101	12.0	−3	106	8.5	16	?	A/H
15-1, 105	125.55	2	359	4.5	−8	355	1.2	16	?	A/H
15-2, 55	126.55	68	250	4.9	65	292	3.4	13	N	A
15-3, 52	128.02	16	115	5.9	14	117	2.8	16	N	A
15-4, 55	129.55	14	248	2.3	13	234	1.1	10	N	B
15-5, 16	130.66	36	55	2.9	19	73	2.3	16	N	A
15-5, 90	131.40	35	133	4.2	40	138	2.5	16	N	A
15-6, 16	132.16	20	95	5.9	14	109	1.1	16	N	A
16-2, 58	136.08	32	184	5.0	−16	32	0.55	40	R?	C−
16-2, 138	136.88	3	312	10.9	−14	304	3.1	30	R	A
16-3, 58	137.58	58	269	1.4	−34	324	0.35	30	R	C
16-4, 31	138.89	34	241	1.0	−4	215	0.62	30	?	A/H
16-4, 100	139.50	53	173	0.93	12	322	0.63	30	N?	C+
16-5, 47	140.47	4	54	5.4	9	321	0.98	25	N?	C
16-6, 88	142.38	−15	231	2.2	−32	196	0.66	25	R	A
17-1, 42	143.92	−5	338	9.1	−12	272	1.9	16	R	C
17-2, 128	146.28	32	169	1.9	−23	48	0.78	25	R	C+
17-3, 28	146.78	9	50	3.8	−20	21	3.0	13	R	A
17-3, 102	147.52	−6	158	0.30	−24	55	0.20	20	R	C+
17-4, 74	148.74	8	130	2.2	−23	79	0.71	30	R	C+
18-1, 39	153.39	17	85	4.8	2	36	1.4	16		
s 0 d 20		3	83		−17	36			R	A
18-1, 141	154.41	13	255	14.4	−34	281	4.3	30	R	A
18-3, 56	156.56	56	299	1.5	50	338	0.62	45		
s 180 d 20		38	289		40	320			N	C
18-4, 116	158.56	23	94	5.9	70	49	0.95	50		
s 0 d 20		3	94		51	67			N	C+
18-5, 133	160.33	60	125	5.1	48	183	1.7	23		
s 0 d 20		42	113		45	162			N	A
18-6, 75	161.25	10	108	4.7	−10	120	0.35	26	R	A
19-1, 77	163.27	20	332	2.1	4	358	1.4	16		
s 130 d 40		30	314		32	348			N	A
19-1, 146	163.96	43	116	0.2	6	303	0.14	25		
s 0 d 25					27	308			N?	C
19-6, 110	171.10	10	193	35.7	13	213	11.6	25		
s 0 d 10		13	191		18	210			N	A
20-1, 35	172.35	−52	92	0.25	−10	40	0.80	40	R	A
20-1, 123	173.23	−2	22	2.1	−28	326	0.48	50	R	C+
20-3, 81	175.81	−8	22	0.57	0	329	0.80	30	?	A/H
20-4, 141	177.91	−14	327	3.5	−13	329	1.7	20	R	A
20-5, 16	178.16	23	263	28.7	20	300	2.9	40	N	C
20-6, 92	180.42	44	43	2.9	60	5	1.7	30	N	A
20-7, 6	181.06	−12	89	1.4	−12	94	1.1	10	R	A
21-1, 9	181.59	29	99	2.8	44	22	1.2	20	N	A−
21-1, 98	182.48	7	166	6.5	−14	137	3.5	20	R	C
21-2, 88	183.88	27	268	15.0	3	300	5.7	25	?	A/H

Table 1A. (Continued).

		NRM			Optimum Demag					
Sample (core-section, cm level)	Sub-bottom depth (m)	Inclination (degrees)	Relative declination (degrees)	Intensity ×10^{-3} (A/m)	Inclination (degrees)	Relative declination (degrees)	Intensity ×10^{-3} (A/m)	Demagnetization level (mT)	Polarity	Reliability[a]
Hole 541 (Cont.)										
21-3, 25	184.75	4	92	3.6	−25	5	2.1	20	R	A
21-3, 102	185.52	11	104	10.5	16	22	1.4	35	N	C+
22-1, 64	191.64	17	292	4.1	20	329	0.70	35		
s 150 d 25					17	320			N	A
22-1, 128	192.28	23	153	4.8	14	145	0.49	40	N	A−
22-2, 62	193.12	31	230	8.3	32	289	1.9	30	N	A
22-3, 58	194.58	24	92	5.2	13	341	1.9	25	N	A
22-4, 7	195.57	−16	260	50.5	−28	254	23.5	35	R	A
22-4, 128	196.78	7	84	3.7	−34	351	1.6	30	R	A
22-5, 60	197.60	−44	116	0.80	4	358	0.26	30	?	A/H
22-6, 42	198.92	0	83	0.88	−20	21	0.48	25	R	A
22-6, 130	199.80	−2	18	15.9	−32	325	7.4	25	R	A
23-1, 78	201.28	−15	87	4.6	20	46	1.8	16		
s 310 d 15		4	85		5	46			?	A/H
23-5, 35	207.28	8	316	7.1	−16	336	0.81	60		
s 150 d 40		0	312		−8	345			R?	A−/H
23-6, 94	208.94	1	5	39.5	3	5	19.2	20	?	A/H
32-3, 29	289.29	5	53	6.2	14	314	0.95	23		
s 210 d 45		20	43		−30	315			R	A−
33-5, 11	301.61	41	267	22.6	4	149	8.2	23	?	A/H
33-6, 15	303.15	35	204	9.8	7	154	0.60	20		
s 0 d 20		41	189		−2	153			?	C/H
33-6, 75	303.75	39	177	4.6	42	161	0.95	13		
s 50 d 45		0	168		−4	157			?	A/H
33-7, 45	304.95	8	137	0.3	53	217	0.13	35		
s 150 d 25		12	142		29	224			N	A−
34-1, 32	305.32	57	309	20.3	3	77	19.1	26		
s 60 d 30		79	248		−6	76			?	A/H
34-5, 67	311.67	36	243	75.9	21	190	6.0	30		
s 90 d 20		25	233		2	189			?	C/H
34-6, 46	312.96	36	310	45.7	67	223	6.4	30		
s 180 d 30		12	302		42	248			N	C
35-5, 66	321.16	32	164	7.7	0	104	1.5	26		
s 40 d 45		−7	159		−39	95			R	C
37-2, 109	336.09	4	86	0.64	−7	333	0.10	25		
s 200 d 20		22	84		−21	336			R?	D
37-3, 81	337.31	18	121	1.0	−12	67	0.9	30		
s 330 d 25		5	117		−37	69			R	A
37-5, 78	340.28	18	183	11.1	18	193	4.9	30		
s 0 d 15		18	178		21	188			N	A
41-4, 57	376.57	23	122	9.2	10	60	2.6	16	N?	C
41-4, 107	377.07	36	146	14.5	16	91	5.2	16	N	C
42-1, 103	382.03	36	276	43.5	35	283	26.1	16	N	A
42-2, 98	383.48	36	214	47.8	37	220	23.3	16	N	A
42-3, 106	385.06	36	105	18.8	−9	20	3.2	30	R?	C
42-4, 64	386.14	23	65	27.2	23	68	13.3	16	N	B
42-5, 3	387.03	33	358	29.3	34	322	8.5	16	N	B
43-5, 69	397.19	41	328	66.0	31	327	27.0	10		
s 120 d 125		−5	252		1	259			?	A/H
43-5, 77	397.27	24	108	59.3	20	113	41.0	10		
s ? d 125									?	A
43-6, 109	399.09	27	222	63.6	25	228	28.6	16	N	B
44-4, 148	405.98	32	67	18.9	−36	331	3.7	45	R	C
44-5, 78	406.78	28	40	118.8	24	40	86.5	10	N	B
44-6, 82	408.32	32	174	47.1	38	142	7.6	25	N	C
44-7, 55	409.55	40	136	86.2	32	132	57.4	10	N	B
45-1, 141	410.91	39	358	19.2	32	2	13.4	10	N	B
45-2, 27	411.27	27	297	98.7	31	304	64.6	10	N	B
45-3, 61	413.11	38	62	68.7	38	57	46.4	10	N	B
45-7, 17	418.67	37	255	18.3	36	259	13.5	10	N	B
48-4, 10	442.60	2	260	9.7	−6	284	0.3	16	?	C
48-4, 108	443.58		41	12.3	50	44	7.2	10	N	B
48-6, 65	446.15	12	349	25.5	0	336	10.0	16	?	C
48-6, 102	446.52	−21	232	18.6	−15	230	11.7	10	R	B
48,CC (15)	447.65	11	135	7.5	−56	258	0.6	16	??	F
49-2, 115	450.15	15	66	17.6	6	85	1.8	13	?	A/H
49-2, 129	450.29				−6	227	3.4	16		
49-3, 42	450.92	23	80	1.2	13	93	0.5	13	N?	C
49-4, 32	452.32	33	167	18.1	25	149	9.6	16	N	C
49-4, 138	453.38	16	302	20.5	6	286	9.0	16	?	C
49-5, 52	454.02	66	333	8.6						
Hole 542										
H2-2, 108		−19	186	0.91	−7	237	0.40	5	?	C
H2-7, 98		4	124	12.5	0	120	5.9	16	?	A/H
H3-1, 145		−13	117	48.3	−11	108	30.7	16		
s 300 d 25		−13	123		−14	114			R	A
H3-3, 97		−11	133	4.1	−8	143	0.96	10	R?	A
1-1, 14	202.14	23	337	12.7	17	344	2.1	10	N	B
1-2, 99	204.49	−18	109	18.8	−10	97	18.9	16	R	A
1-3, 52	205.52	−36	135	46.1	−36	131	32.9	10	R	B
1-4, 35	206.85	−13	281	39.0	−15	263	18.8	16	R	A
1-4, 103	207.53	23	49	0.77	−9	316	0.18	50		
s 330 d 12					−6	314			?	C/H
1-6, 69	210.19	11	76	25.1	4	89	5.4	16	?	A/H
2-2, 119	214.19	−36	337	12.4	22	59	4.2	16	N	C

Table 1A. (Continued).

		NRM			Optimum Demag					
Sample (core-section, cm level)	Sub-bottom depth (m)	Incli-nation (degrees)	Relative decli-nation (degrees)	Intensity $\times 10^{-3}$ (A/m)	Incli-nation (degrees)	Relative decli-nation (degrees)	Intensity $\times 10^{-3}$ (A/m)	Demagne-tization level (mT)	Polarity	Relia-bility[a]
Hole 542 (Cont.)										
2-3, 50	215.00	−54	94	0.74	−46	94	0.40	5	R?	C
2-5, 100	218.50	14	44	11.0	10	59	1.2	16	N	A
3-2, 95	223.95	−40	176	12.0	−28	185	7.7	16		
s 0 d 10					−29	190			R	A
3-3, 67	224.67	−20	93	2.2	−21	101	1.8	10		
s 30 d 10		−28	91		−30	100			R	A
3-5, 120	228.20	−43	136	0.95	−38	329	0.09	15		
s 0 d 20		−55	155		−26	319			R	C
3-6, 38	228.88	−35	110	1.7	12	348	0.05	40		
s 180 d 10		−25	108		9	347			?	C
4-1, 42	230.92	−22	99	2.6	−12	292	0.27	25		
s 150 d 30		1	96		−29	302			R	C
4-5, 55	237.05	8	134	8.8	19	124	2.3	13		
s 180 d 18		20	130		33	130			N	A
Hole 542A										
2-4, 132	245.82	16	306	18.4	19	302	12.6	16		
s 300 d 25		12	312		16	310			N	A+
2-6, 76	248.26	−62	80	12.0	−54	138	14.0	20		
s 300 d 35		−64	156		−34	167			R	A+
3-2, 25	251.25	25	331	15.7	30	330	11.8	16		
s 340 d 25		27	341		32	342			N	A+
3-6, 72	257.72	6	269	10.2	7	267	3.8	13		
s 0 d 18		24	269		24	266			N	A+
4-1, 32	259.32	−26	162	26.3	−26	156	26.6	16	R	A
4-1, 82	259.82	20	295	20.3	36	287	2.6	16	N	C
4-4, 108	264.58	−49	347	2.5	−38	197	2.7	20		
s 40 d 15		−36	340		−42	209			R	A+
Hole 543										
6-6, 142	57.42	−38	40	3.8	−45	34	2.4	16	R	A
7-4, 8	62.58	−11	115	9.1	−20	99	5.6	16	R	A
8-5, 123	74.73	−11	173	4.7	−12	166	6.0	16	R	A
9-3, 22	80.22	15	110	2.3	−9	151	1.4	16	R?	A
10-5, 33	92.83	24	36	11.6	15	42	5.2	16	N	A
11-3, 133	100.33	24	12	4.5	7	12	3.3	25	?	C
12-1, 8	105.58	−23	351	4.6	−29	310	2.0	13	R	C
12-1, 48	105.98	−53	250	4.6	−28	271	5.1	16	R	A
13-2, 19	116.69	11	278	7.1	12	277	5.1	16	N	A
13-3, 131	119.31	40	105	0.5	15	27	5.8	20	N	C
13-5, 125	122.25	26	105	2.4	14	10	3.4	20	N?	C
14-1, 7	124.57	4	45	11.4	−5	16	6.3	30	?	C
14-2, 139	127.39	12	291	1.6	9	333	5.2	25	?	C
15-2, 5	135.55	−70	203	3.5	3	323	3.8	30	?	C
17-1, 138	154.38	35	80	8.2	34	95	1.8	16	N	A
17-2, 99	155.49	4	53	1.6	−20	23	2.5	16	R	A
17-3, 32	156.32	10	352	8.7	0	336	1.7	20	?	A/H
17-4, 16	157.66	27	306	8.9	22	312	1.5	16	N	A
17-4, 141	158.91	60	331	2.8	39	331	1.1	20	N	C
18-1, 35	162.85	34	318	10.6	21	319	2.3	16	N	A
18-2, 113	165.13	26	346	0.6	40	12	0.5	13	N	C
18-3, 126	166.76	47	224	10.2	40	208	3.2	16	N	A
18-4, 53	167.53	64	67	3.5	−18	184	0.9	25	R	C
18-6, 93	170.93	−8	116	1.7	−25	113	4.8	20	R	A
19-1, 78	172.78	38	323	3.8	−13	216	0.7	20	R?	C
19-3, 26	175.26	8	349	3.5	10	334	1.0	16	N	A
19-4, 80	177.30	61	196	5.7	44	219	1.0	13	N	A
19-5, 92	178.92	42	89	2.9	36	115	0.34	20	N	A
19-7, 3	181.03	−5	273	1.4	−22	244	0.52	13	R	A
20-1, 89	182.39	−14	218	1.9	−39	206	3.4	16	R	C
20-2, 52	183.52	−44	42	0.9	−70	19	0.57	13	R	C
20-3, 27	184.77	36	65	10.5	19	69	1.9	16	N	A
20-3, 113	185.63	31	35	1.4	−28	358	1.7	16	R	C
20-4, 18	186.18	−1	358	2.4	−32	258	1.9	16	R	A
20-4, 122	187.22	37	323	8.1	6	337	1.1	25	?	C/H
23-2, 139	212.89	15	118	1.0	−5	153	0.79	20	?	C/H
23-3, 23	213.23	33	250	1.6	26	243	0.72	16	N	A
24-2, 144	222.44	−66	321	0.42	−71	340	0.40	13	R	A−
24-4, 18	224.18	−31	312	0.55	−67	4	0.30	13	R	C
24-4, 98	224.98	−71	245	0.24	−13	24	0.08	20	R?	C
25-1, 48	229.48	−68	352	0.32	−59	325	0.36	13	R	C
25-2, 49	230.99	−18	28	1.6	−30	294	0.25	16	R	C
25-2, 115	231.65	9	339	3.1	−38	246	0.87	16	R	A
25-3, 29	232.29	25	330	1.6	−19	195	0.78	16	R	C
26-2, 46	240.46	56	356	2.9	1	335	2.3	20	?	C/H
26-2, 114	241.14	49	263	4.2	−34	103	1.4	16	R	A
26-3, 35	241.85	−15	319	2.7	7	285	0.43	25	?	A/H
26-3, 85	242.35	37	190	3.3	−34	98	0.57	16	R	C
26-4, 43	243.43	46	181	3.1	−19	13	0.74	13	R	A
26-4, 103	244.03	20	18	4.0	−4	349	0.16	25	?	C−
26-5, 73	245.23	62	104	3.6	−24	312	1.4	16	R	A
26-6, 44	246.44	28	13	2.1	−3	198	0.57	20	?	A/H
26-6, 121	247.21	73	77	2.1	−34	353	1.1	13	R	C
27-2, 121	250.71	31	297	3.8	−9	126	2.4	16	R	A
27-3, 39	251.39	38	344	3.2	−73	215	0.43	16	R	A

Table 1A. (Continued).

Sample (core-section, cm level)	Sub-bottom depth (m)	NRM			Optimum Demag					
		Inclination (degrees)	Relative declination (degrees)	Intensity ×10^{-3} (A/m)	Inclination (degrees)	Relative declination (degrees)	Intensity ×10^{-3} (A/m)	Demagnetization level (mT)	Polarity	Reliability[a]
Hole 543 (Cont.)										
27-4, 113	253.63	69	79	4.6	−21	300	1.4	16	R	A
27-5, 4	254.04	66	60	4.2	−15	292	2.1	16	R	A
28-2, 27	259.27	30	191	10.6	−11	190	1.8	35	R	C
28-3, 27	260.77	43	40	7.5	22	84	0.54	20	N	A
28-3, 131	261.81	19	307	6.6	−26	313	0.30	16	R	C
28-4, 38	262.38	26	19	7.9	−40	350	0.2	16	R?	D
28-4, 94	262.94	19	333	7.8	−33	182	0.16	16	R?	D
28-5, 54	264.04	32	236	7.2	−1	217	1.6	25	?	A/H
29-1, 111	268.11	18	336	7.8	−14	327	1.8	20	R	C
29-2, 111	269.61	66	204	4.6	−10	10	1.7	20	R	A
29-3, 24	270.24	44	343	5.2	−35	183	0.55	16	R	C
29-3, 111	271.11	27	24	5.1	−16	203	0.54	13	R	C
29-4, 111	272.61	30	340	3.6	−17	242	0.41	20	R	C+
29-5, 111	274.11	80	56	2.3	−10	253	3.3	16	R	C
29-6, 24	274.74	35	3	1.6	7	308	0.17	30	?	C
29-6, 111	275.61	36	168	6.8	−7	172	1.3	20	R?	C
29-7, 20	276.20	1	91	4.4	5	102	1.2	20	?	A/H
30-1, 99	277.49	18	34	10.0	−4	36	1.4	20	?	A/H
30-2, 94	278.94	29	334	5.4	−83	325	0.32	16	R?	D
30-3, 93	280.43	19	26	5.6	−5	73	1.0	20	?	A/H
30-4, 105	282.05	−10	31	3.9	−5	231	1.3	20	?	A/H
30-5, 107	283.57	60	14	4.2	−14	346	0.95	25	R	A
30-6, 56	284.56	85	310	4.8	−13	292	2.3	16	R	A
31-1, 32	286.32	27	264	6.7	−11	245	1.1	16	R	A
31-2, 14	287.64	25	53	5.9	−15	58	0.82	20	R	C
32-1, 91	296.41	42	248	1.2	11	63	0.46	16	N?	C
32-2, 103	298.03	−11	285	1.3	−18	282	1.7	16	R	A
32-3, 92	299.42	5	280	0.79	−13	245	0.74	16	R	C
32-4, 122	301.22	−6	115	1.0	−20	121	1.4	16	R	A
32-5, 89	302.39	−59	351	0.62	−71	52	0.82	13	R	A−
33-1, 94	305.94	14	181	2.5	1	187	1.4	25	?	A/H
33-2, 70	307.20	8	266	2.6	−10	267	1.5	25	R	C
34-1, 102	315.52	−25	133	1.5	−25	128	1.4	16	R	A+
34-2, 23	316.23	−61	266	1.1	−59	271	1.2	16	R	A+
Hole 543A										
3-1, 3	341.53	21	218	4.6	6	206	2.0	20	?	A+/H
3-1, 40	341.90	32	69	3.6	9	152	1.1	25	N?	A+/H
5-1, 104	361.54	−26	337	4.3	−58	166	1.1	25	R	A
5-2, 81	362.81	5	326	5.3	−9	326	0.28	25	R?	C+/H
5-3, 94	364.44	11	16	11.2	17	39	1.3	25	N	A+
6-1, 18	370.18	25	303	3.9	−4	311	0.47	40	?	C/H
7-2, 103	382.03	20	342	11.7	35	262	0.46	20	N	A−
7-3, 7	382.57	48	290	0.39	31	157	0.09	35	N	C
7-3, 14	382.64	−5	358	12.3	−23	335	1.2	25	R	A
7-3, 85	383.35	17	6	18.6	39	17	1.5	25	N	A−
8-1, 76	389.76	−15	33	11.0	−31	354	2.5	20	R	A
9-1, 46	398.96	4	351	23.1	−48	33	0.63	20	?	F
10-1, 11	408.11	52	75	5.3	24	156	3.3	25	N	A

Note: For samples from dipping beds, a second line of data gives strike (s), dip (d), and corrected inclinations and declinations.
[a] Reliability categories: A = stable, multiple demagnetizations; B = stable, single demagnetization; C = direction changing systematically at highest demagnetization level; D = marginally stable; F = unstable; H = too close to horizontal for polarity determination. (See text.)

few confident polarity determinations were too far apart for polarity stratigraphy. The samples from 382 to 419 m (Cores 42 to 44) at first looked promising. Fourteen of 15 samples have inclinations between 21° and 38° (without tectonic correction), and all of these samples have very high intensities and show exceptional directional stability. However, applying the tectonic correction to the two samples from the overturned section in Section 43-5 results in nearly horizontal magnetizations, strongly suggesting a post-deformational magnetization. This interpretation is supported by the failure to observe similar properties of intensity or stability in any samples that might be the same age at Site 543. The most likely mechanism for resetting the magnetization is chemical or thermal changes associated with the warm water observed at the bottom of the hole.

Site 542

The number of sediment specimens available from Site 542 was inadequate for polarity stratigraphy, even though the samples were quite stable and horizontal magnetizations were rare. In Hole 542, the predominantly reversed interval from 200 to 230 m (Cores 1 to 4) probably corresponds to the Gilbert epoch, but this assignment is based more on the nannofossil age than on the polarity intervals.

Site 543

At Site 543, drilling deformation prevented adequate sampling of the sediments in the upper 150 m (Hole 543, Cores 1 to 16). Sampling was adequate in Cores 17 to 20 (150–190 m), and a correlation can be drawn with Anomalies 5C through 5E (16 to 19 Ma) of the reversal time scale (Fig. 3). This is in agreement with the radiolarian age assignments of *D. alata* to *S. wolffii* (see Site Report for Site 543, this volume) based on the time scale of Theyer and Hammond (1974). Cores 21 and 22 had no recovery, and Cores 23 through 34 (the bottom of Hole 543) show a dramatic change in directional properties. The vast majority of the samples have reversed sta-

Table 1B. Basalt paleomagnetic data, Hole 543A.

		NRM			Optimum Demag				
Sample (core-section, cm level)	Sub-bottom depth (m)	Incli-nation (degrees)	Relative decli-nation (degrees)	Intensity (A/m)	Incli-nation (degrees)	Relative decli-nation (degrees)	Intensity (A/m)	Demagne-tization level (mT)	Susceptibility (10^{-4} cgs)
10-1, 127	409.27	−11.1	163.1	2.71	−11.8	161.4	1.82	20	3.1
10-2, 32	409.82	−29.5	268.7	5.74	−29.4	270.2	3.95	20	7.6
11-1, 40	417.90	−36.9	359.1	5.16	−35.9	0.1	3.71	450°C[a]	6.1
11-1, 140	418.90	−34.9	272.5	8.56	−32.5	274.1	5.05	20	7.2
11-2, 85	419.85	−28.8	198.2	5.16	−30.8	198.6	2.28	20	9.1
12-1, 32	420.32	−31.9	210.6	8.25	−31.8	211.6	4.74	450°C	6.8
12-2, 6	421.56	−20.5	139.1	7.56	−20.9	135.6	4.45	20	10.0
12-2, 64	422.14	−19.3	202.9	6.76	−19.8	204.2	3.09	20	8.3
12-3, 40	423.40	−21.9	107.1	4.06	−23.7	107.8	2.82	20	
12-4, 135	425.85	−21.6	132.0	5.33	−20.9	130.9	3.66	20	6.1
13-1, 26	427.26	−21.4	88.6	6.70	−21.0	88.4	5.74	20	3.2
13-2, 93	429.43	−22.1	211.9	5.41					
13-3, 74	430.74	−32.7	234.2	5.03	−31.4	238.3	1.37	20	12.3
13-5, 40	433.40	−27.9	4.0	9.67	−27.8	7.5	6.42	340°C	6.8
13-6, 114	435.64	—23.7	276.5	6.12	−24.0	276.4	2.14	20	10.7
13-7, 42	436.42	−26.2	172.0	6.10	−24.4	168.3	0.89	20	16.8
14-1, 28	436.28	−23.6	90.3	6.94	−19.2	86.2	1.29	20	12.8
15-1, 35	438.35	−25.4	335.3	14.5	−26.4	335.8	10.9	340°C	6.0
15-2, 14	439.64	−28.8	250.3	5.56	−27.1	255.6	1.25	20	13.7
15-3, 70	441.70	−22.5	196.4	10.6	−21.2	197.4	2.95	20	11.2
15-4, 117	443.67	−27.7	224.2	8.35	−28.3	229.9	2.38	20	10.4
15-5, 65	444.65	−23.2	177.7	7.95	−23.2	177.2	2.72	20	9.2
16-1, 94	445.94	−28.0	232.4	8.98	−27.7	235.1	3.99	20	8.5
16-2, 38	446.88	−20.7	96.2	9.47	−19.3	94.4	4.11	20	7.8
16-3, 127	449.27	−21.7	180.5	9.01	−20.8	180.5	2.39	20	10.6
16-4, 91	450.41	−21.5	145.8	9.23	−19.6	144.3	2.52	20	9.7
16-5, 78	451.78	−17.9	191.1	10.5	−19.4	191.5	2.53	20	11.2
16-6, 88	453.38	−21.1	14.1	10.9	−22.8	14.1	5.18	340°C	5.1
16-7, 86	454.86	−32.9	272.4	5.70	−31.5	273.6	3.16	20	6.6

Note: See Table 1A footnotes for reliability catetories and other information.
[a] Temperature of thermal demagnetization.

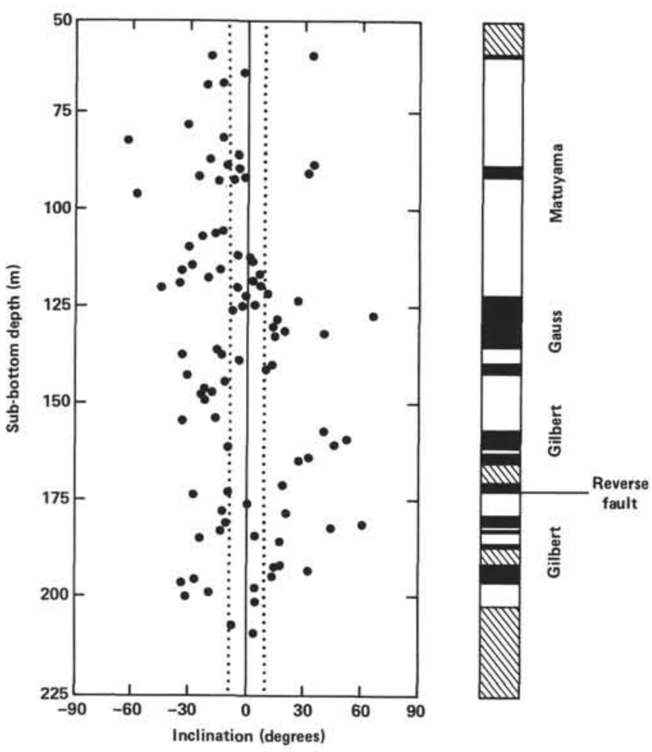

Figure 2. Inclinations and polarity interpretations for Site 541. The dotted lines indicate the 10° cutoff for polarity determinations. Black indicates normal polarity; white, reversed; and hachured, indeterminate.

ble directions, though most have normal NRM's. Since the age range of these samples covers most of the Eocene and Oligocene, some type of post-depositional remagnetization is clearly indicated. A likely cause of the remagnetization is the diagenetic changes associated with the formation of manganese staining and of authigenic rhodochrosite. There is very little information as to the age of this remagnetization.

The Paleocene(?) and Upper Cretaceous sediments of Hole 543A were only sparsely sampled, owing to drilling deformation. Polarities are mixed; about a third of the samples have nearly horizontal magnetization. The age of magnetization of these iron-rich sediments is open to question, however, since reddish staining fronts were observed to crosscut bedding features.

STRUCTURAL INTERPRETATION

The interpretation of *in situ* structure provided interesting results. The objective is to use the magnetic declination of samples taken at dipping beds to estimate the original orientation and thereby determine approximately the true dip directions of the beds. Of the samples collected at dipping beds for Site 541, twelve have very stable directions, and eight of these have unambiguous polarity. For Site 542, nine samples at apparently dipping beds have very stable magnetizations. However, Hole 542 was abandoned because it was measured to deviate 7.6° from vertical, so three samples with only moderate dips from this hole have been excluded. For the samples with clearly determined polarity, true north was assumed to be the declination direction for normal samples, and declination minus 180° for reversed rocks. The apparent *in situ* strikes and down-dip directions in Table 2 and Figure 4 are relative to this north. For any one sample, the uncertainty in this rather crude technique is estimated to be about 40°. The main sources of error are the lack of

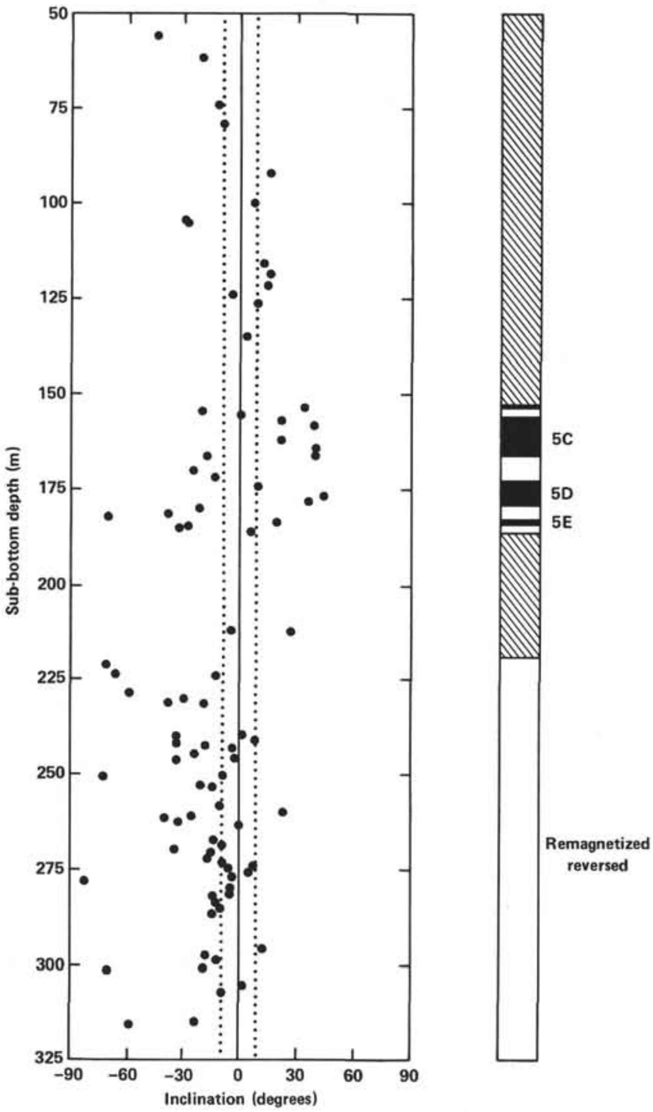

Figure 3. Inclinations and polarity interpretations for Site 543. Symbols as in Figure 2.

Table 2. Structural interpretation.

Sample (core-section, cm level)	Bedding (relative to core) Strike (degrees)	Bedding (relative to core) Dip (degrees)	Magnetization (corrected for bedding) Incli-nation (degrees)	Magnetization (corrected for bedding) Decli-nation (degrees)	Polarity	Apparent *in situ* down-dip direction (degrees)
Hole 541						
18-1, 39	300	20	−17	36	R	174
18-5, 133	0	20	45	162	N	288
19-1, 77	130	40	32	348	N	232
19-6, 110	0	10	18	210	N	240
22-1, 64	150	25	17	320	N	280
32-3, 29	210	45	−30	315	R	165
37-3, 81	330	25	−37	69	R	171
37-5, 78	0	15	21	188	N	262
Polarity ambiguous						
23-1, 78	310	15	5	46		174 or 354
23-5, 78	150	40	4	317		103 or 283
33-6, 75	50	45	−4	157		103 or 283
34-1, 32	60	30	−6	76		74 or 254
Hole 542						
H3-1, 145	300	25	−14	114	R	96
Hole 542A						
2-4, 132	300	25	16	310	N	80
2-6, 76	300	35	−34	167	R	43
3-2, 25	340	25	32	342	N	88
3-6, 72	0	18	24	266	N	184
4-4, 108	40	15	−42	209	R	101

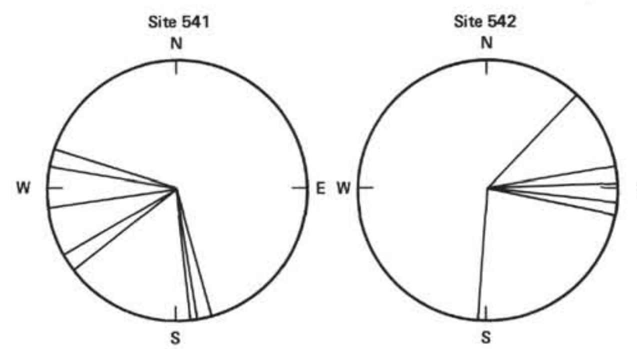

Figure 4. Estimates of *in situ* down-dip direction, based on the difference between magnetic declination and bedding strike relative to the core. Each radial line represents the down-dip direction for a single bed.

correspondence between the declination direction and true north, and the uncertainty in measuring the orientation of a slightly deformed bed on half of a 10-cm-diameter core. From Site 541, the eight samples with clear polarity scatter about dip directions to the southwest, and the samples with ambiguous polarity are not inconsistent with this. For Site 542, located about 1.5 km to the east, the six samples dip predominantly to the east. The scatter within each site is remarkably small, considering the uncertainties. These dipping beds, often with dips of 30° to 45°, alternate with horizontal beds over depth ranges of typically 5 to 10 m. The *in situ* pattern suggested by horizontal beds alternating with dipping beds with the same down-dip direction is that the regions of horizontal bedding are separated by bands of monoclinal folds, with the axial plane of the folds probably dipping in the opposite direction from the bedding dip. These fold bands may well be controlled by subparallel thrust faults.

BASALT MAGNETIZATION

Coring of Hole 543A recovered 35.9 m of basalt at an average recovery rate of 81%. The lithology was moderately altered plagioclase–olivine phyric pillow basalt. These flows are dated as Campanian (approx 80 Ma old) on the basis of overlying and interbedded sediment, and compositionally are typical of normal ocean crust (e.g., Bougault et al., this volume). The freedom from limitation of the sample interval and the high degree of magnetic stability provided a pleasant contrast to the sedimentary section. The sample interval averaged about 1.5 m, and the remanence direction rarely moved more than 3° to 4° during either AF or thermal demagnetization. There is no indication of drilling-induced, viscous, or other type of unstable magnetization. The samples from Hole 543A can be divided into three groups according to their inclinations: group 1 consists of a single sample from Section 10-1 (409 m), with an inclination of −11°; group 2 includes Sections 10-2 to 12-1 (410–420 m), with inclinations of −29° to −36°; and group 3 includes Sections 12-2 to 16-7 (421–455 m), with inclinations of −19° to −31°. These groupings are very similar to those based on petrography (Natland et al., this volume). The interpretation of these distinct mineralogic and magnetic groups is that they represent brief eruptive events separated by fairly long time intervals.

The mean NRM intensity of the basalt samples is 7.45 A/m, with a standard deviation of 2.50. Using the results from Sites 417 and 418 (Levi et al., 1979) as a standard for Cretaceous basalts, these intensities fall well within the normal scatter. The mean susceptibility is 8.8×10^{-4} cgs units, with standard deviation 3.1×10^{-4}. This is again within the normal range, perhaps below average. The Königsberger ratio Q of remanent to induced magnetization scatters between 10 and 50; most values are near 20. The median destructive fields determined from AF demagnetizations range from 10 to 25 mT; again, these values are not unusual.

SUMMARY

Magnetostratigraphy for Leg 78A met with limited success. For Site 541, the interval from 60 to 200 m was correlated with the Matuyama through Gilbert polarity epochs. For Site 543, the interval from 150 to 190 m was correlated with marine magnetic Anomalies 5C through 5E. Down-dip directions of tilted beds inferred from declination values for Sites 541 and 542 suggest a pattern of monoclinal folding. Results from basalts are comparable to those for other DSDP sites.

ACKNOWLEDGMENTS

Reviews by Shaul Levi and Fritz Theyer improved the manuscript.

REFERENCES

Levi, S., Bleil, U., Smith, B. M., and Rigotti, P. A., 1979. Compilation of paleomagnetic and rock magnetic results of basalt samples from DSDP Legs 51, 52, and 53. *In* Donnelly, T., Francheteau, J., Bryan, W., Robinson, P., Flower, M., Salisbury, M., et al., *Init. Repts. DSDP,* 51, 52, 53, Pt. 2: Washington (U.S. Govt. Printing Office), 1337–1350.

Ness, G., Levi, S., and Couch, R., 1980. Marine magnetic anomaly timescales for the Cenozoic and Late Cretaceous: a précis, critique, and synthesis. *Rev. Geophys. Space Phys.,* 18:753–770.

Theyer, F., and Hammond, S. R., 1974. Paleomagnetic polarity sequence and radiolarian zones, Brunhes to polarity epoch 20. *Earth Planet. Sci. Lett.,* 22:307–319.

Date of Initial Receipt: July 25, 1983
Date of Acceptance: August 19, 1983